Differences between pressure-induced densification of LiCl–H$_2$O glass and polyamorphic transition of H$_2$O

Yoshiharu Suzuki and Osamu Mishima

Polyamorphism Group, Advanced Nano Materials Laboratory, National Institute for Materials
Science, Namiki 1-1, Tsukuba, Ibaraki, 305-0044, Japan

E-mail: SUZUKI.Yoshiharu@nims.go.jp

Abstract

We perform volumetric measurements of LiCl aqueous solution up to 1.00 GPa in the
100–170 K range, examine the pressure-induced vitrification and densification, and draw the
pressure–temperature–volume surface. The pressure-induced vitrification of the solution
corresponds to the cooling-induced vitrification of the liquid. We found that the volumetric
decrease of glassy solution during the densification is continuous and this behavior depends on
the glassy state before the compression. Raman profiles of the glassy solutions before and after
the densification are similar. In contrast, the polyamorphic transition from low-density
amorphous ice (LDA) to high-density amorphous ice (HDA) is discontinuous and their Raman
profile before and after the transition is distinct. These results suggest that the densification
relates to the structural relaxation and differs intrinsically from the polyamorphic transition.

Furthermore, the densification of HDA is observed under high pressure, suggesting that
very high-density amorphous ice (VHDA) may be the densified HDA. In order to recognize a
polyamorphic transition under a non-equilibrium condition correctly, evidence of not only large
volume change but also some distinct structural changes in glassy state is necessary.

1. Introduction

We can regard glass as an out-of-equilibrium liquid that
may inherit a liquid structure just before the vitrification [1].
Because of its long structural relaxation time, it is possible
to form various glassy states by changing the glass formation
condition. Therefore, it is usually difficult to control the glassy
state, and the nature of glass is hardly understood.

We are interested in two pressure effects on glass. One
is the pressure-induced densification of glass. Although
the densification of SiO$_2$ glass has been reported since
1953 [2–4], there exists almost no thorough investigation of the
densification. Another is the polyamorphic transition, which
means a discontinuous transition between different amorphous
phases [5–8]. In the case of water polyamorphism [8], low-
and high-density amorphous ices, LDA and HDA respectively,
exist at low temperatures. The transition between LDA
and HDA appears first order. However, the validity of
water polyamorphism has not been yet verified experimentally
because of the non-equilibrium nature.

The densification and the polyamorphic transition are
similar in a sense that a large stepwise volume decrease is
induced by pressure. However, it is not easy to differentiate
between them, because these phenomena occur under non-
equilibrium conditions. In order to save confusion between
them, it is necessary to clarify the difference between both
phenomena. In this study, we compare the densification
of glassy lithium chloride aqueous solution (glassy LiCl$_{aq}$
solution) and the LDA–HDA polyamorphic transition and
show that there are evident differences between them.
In particular, we measure an accurate isothermal volume
change of LiCl$_{aq}$ solution in wide pressure–temperature
regions including its liquid and glassy states, examine the
pressure-induced vitrification and densification, and show
the dependences of temperature and annealing on the glass
densification, for the first time.

2. Experimental method and sample

The concentration of LiCl$_{aq}$ solution used in this experiment
is 11.1 mol%. The nature of solvent water in the highly

concentrated LiCl$_{aq}$ solution is different from that of pure water. This solution vitrifies easily at ~138 K and 1 bar at a cooling rate of ~15 K min^{-1} [9–11]. The phase separation to water-rich solution and solute-rich solution, which is observed in the glasses of dilute LiCl$_{aq}$ solution below 10 mol% [12], does not occur in this concentrated solution sample [10].

An indium container, in which the LiCl$_{aq}$ solution is completely sealed up, is placed in a piston–cylinder pressure device to which a heater and thermocouples are attached. This device is cooled by cold nitrogen gas. The sample temperature error is ±~2 K. The change of sample temperature during the densification and vitrification is ±~2 K. The sample is compressed up to 1.00 GPa at 0.15 GPa min^{-1} while the piston displacement is recorded. Subsequently kept at 1.00 GPa for 10 min, the sample is decompressed to 0.02 GPa at 0.15 GPa min^{-1}. The measured pressure has an error attributed to the friction between piston and cylinder. In order to estimate correct sample pressure, we measure the P–V curves of only indium metal on compression and decompression and calculate the average of their P–V curves. We consider that the difference between the averaged P–V curve and the measured P–V curve is equivalent to the error caused by the friction and estimate the correct sample pressure. The absolute and relative errors of sample pressure are ±~0.01 and ±~0.005 GPa, respectively. The sample volume, V, is corrected by subtracting the indium volume and is accurate to within 1.0%.

3. Results and discussion

The pressure–temperature–volume surfaces of LiCl$_{aq}$ solution during compression and subsequent decompression are shown in figure 1. The figures are the main experimental data of this study. Two pressure effects, the pressure-induced vitrification of liquid and the pressure-induced densification of glass, are drawn together.

In figure 2, the changes in V and isothermal compressibility, $\kappa = -1/V(\delta V/\delta P)_T$, of LiCl$_{aq}$ solution at 165 K during compression and decompression are presented. The slope of the P–V curve becomes small suddenly at ~0.50 GPa and the κ begins to become small discontinuously, indicating that the vitrification of the solution occurs at the glass transition pressure, P_g. On decompression, the V and κ follow different paths. At $P_g \sim 0.45$ GPa, which is slightly lower than P_g of the compression process, V increases rapidly and the peak of κ appears. We consider that the delay of P_g during the decompression is caused by the high viscosity of glass, and is similar to the delay of glass transition temperature observed in an isobaric thermal measurement of glass on reheating, as shown in figure 1 [1, 13, 14]. Likewise, the appearance of the peak of κ corresponds to that of a peak of specific heat on reheating [1, 13, 14]. As shown in figures 1 and 3(b), the value of P_g shifts to the higher pressure side with increasing temperature. The temperature dependence of P_g agrees with the results of the pressure-induced vitrification from the liquid phase [9, 13–16].

In figure 3(a), the P–V curves of the glassy LiCl$_{aq}$ solution at 105 K during compression and decompression
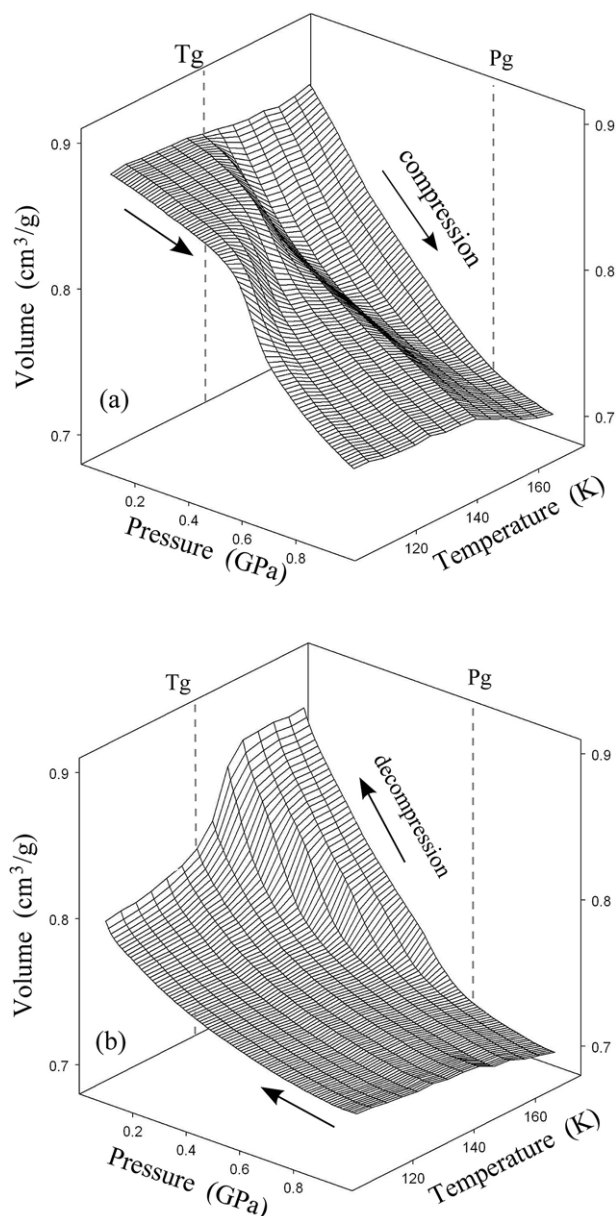

Figure 1. The pressure–temperature–volume surface of 11.1 mol% LiCl aqueous solution during compression (a) and decompression (b). The temperature and pressure range are 100–170 K and 0.02–1.00 GPa. Broken lines stand for the glass transition temperature at 1 bar ($T_g \sim 138$ K) and the glass transition pressure at 170 K ($P_g \sim 0.63$ GPa).

are shown. V decreases more slowly than that of its liquid state until ~0.40 GPa. The glass begins to densify rapidly and continuously around a densification pressure, P_d, of ~0.40 GPa and the slope of the compression curve returns to be small above ~0.6 GPa. As temperature lowers, the P_d value shifts to the higher pressure side (figures 1(a) and 3(b)). On decompression, the V of the densified glassy LiCl$_{aq}$ solution increases monotonically and the V at 1 bar does not return to the original volume before the densification.

In figure 4(a), we show the OH-stretching Raman spectra of glassy solution before and after the densification. All Raman measurements are performed at 77 K and 1 bar. It is difficult
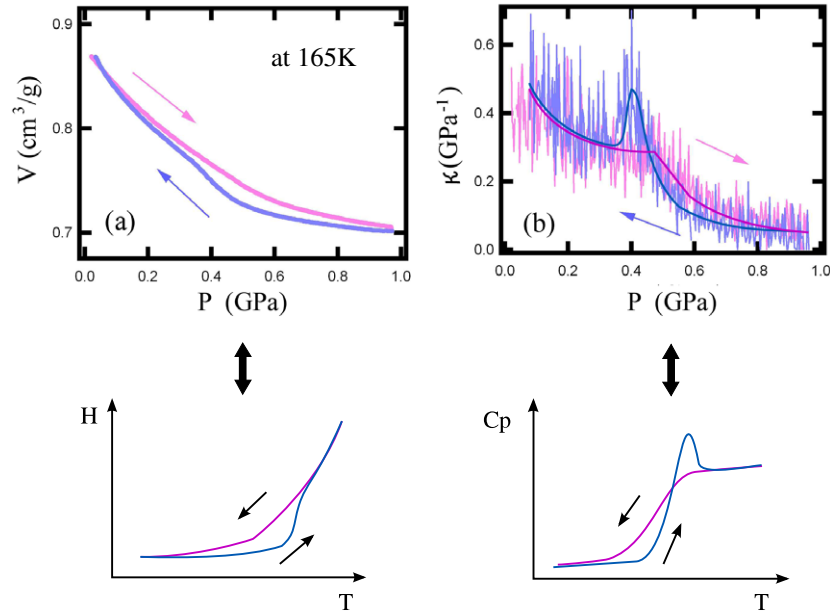
Figure 2. The changes of volume, V, and isothermal compressibility, κ, of LiCl$_{aq}$ solution at 165 K during compression (red) and subsequent decompression (blue). Schematic drawings of the enthalpy, H, and specific heat, C_p, by cooling (red) and subsequently reheating (blue) are presented for comparison. A different path of V on decompression corresponds to that of H on reheating (left), and the appearance of the peak of κ on decompression corresponds to that of C_p on reheating (right).

to disclose the concrete hydrogen-bonded network structure of water molecules in glasses from the analysis of Raman profile because of the complex coupling of several modes. However, we can infer the relative changes of the distance between molecules or of the strength of interaction between molecules from the shift of Raman peak position. In addition, if the drastic change of topological molecular configuration is caused with a first-order phase transition, drastic changes of Raman profile, for example the appearance or disappearance of Raman peaks, would be detected. Although there is a subtle difference between Raman spectra of glassy LiCl$_{aq}$ solution before and after the densification, for example the continuous change of the shoulder at $\sim$3200 cm^{-1} (figure 4(a)), the appearance (or the disappearance) of any new peak is not observed in this spectral range. Their Raman profiles are rather similar. This suggests that the topological configuration of water molecules in the glassy solution is little modified or continuously deformed slightly by the densification.

In figure 5, we show x-ray photos of glassy solution before and after the densification, and cannot find any noticeable differences between them. Unfortunately, because of the low quality and the low resolution of our x-ray equipment, we can only mention that the principal halo pattern is similar to that of liquid water or HDA. Even so, the x-ray photos show that the glassy solutions before and after the densification are in a similar glassy state, as indicated by the above Raman result. The Raman and x-ray results show also that there are no crystalline ices in the glassy LiCl$_{aq}$ solutions.

Next, we investigate the effects of the initial glassy state on the densification. Firstly, we make the densified glassy solutions by 77 K compression, heat them slowly to a certain temperature at 1 bar, and compress them again at 77 K (figure 6(a)). During the annealing, the sample

swells uniformly and continuously and there is neither a drastic change in the Raman profile nor heat evolution relating to crystallization. Therefore, we consider that the volume increase by 1 bar annealing is caused by structural relaxation of the glassy solution. As shown in figure 6(a), the annealed glassy solutions densify broadly and continuously on 77 K compression and their densification behaviors are different, showing different P_d values. The non-annealed glassy sample (marked 2) exhibits no signs of densification during compression.

Secondly, we obtain glassy solution by cooling the liquid at 0.10 GPa. Although the glassy LiCl$_{aq}$ solutions quenched at 0.10 GPa densify in high pressure regions, their P_d values become higher than those of the glassy solutions vitrified at 1 bar (figure 3(b)).

These experimental results show that the glass densification depends strongly on the initial glassy state. This suggests that the glass densification is concerned in the structural relaxation for an approach to the equilibrium state.

In figure 6(b), the $P–V$ curves of LDA at 77 K during compression and decompression are shown for comparison. The V of LDA decreases rapidly and discontinuously at the transition pressure $\sim$ 0.68 GPa. The Raman profile of LDA changes to that of HDA drastically (figure 4(b)). These results indicate that a large modification of molecular configuration occurs at the transition [17]. The discontinuous volume change and the distinctly different Raman profiles differ clearly from the broad and continuous glass densification and the similar Raman profiles of the glassy solutions, respectively.

Recently, we have demonstrated in detail the volume change of HDA during the slow annealing at 1 bar [18]. Firstly, HDA is swollen slowly and uniformly. This uniform and irreversible volume increase can be regarded as the structural
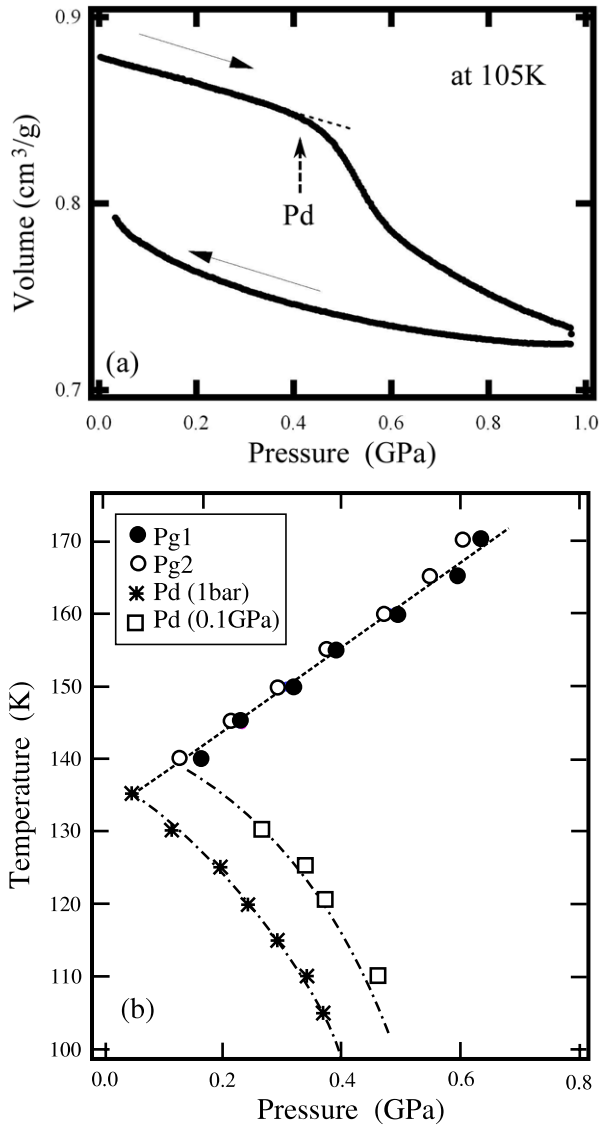
Figure 3. (a) The changes of volume, V, of glassy $LiCl_{aq}$ solution at 105 K during compression and subsequently decompression. P_d stands for the onset of densification. (b) The temperature dependence of P_g and P_d. P_{g1} and P_{g2} stand for P_g during compression and decompression, respectively. P_d of the solution vitrified at 0.10 GPa (square) is higher than P_d of the solution vitrified at 1 bar (asterisk).

Figure 4. The Raman spectra of the OH-stretching vibrational mode of the glassy $LiCl_{aq}$ solutions and amorphous ices. (a) The Raman spectra of glassy $LiCl_{aq}$ solutions before and after the densification is measured at 77 K and 1 bar. (b) The Raman spectra of amorphous ices before and after the polyamorphic transition (LDA and HDA, respectively) is measured at 77 K and 1 bar.

relaxation of HDA because of no large change in Raman profile of HDA. As HDA is annealed further, a local portion of the HDA begins to transform to LDA and its volume increases non-uniformly. Therefore, the HDA and LDA components coexist in the annealed sample and its Raman spectrum can be represented by a linear combination with Raman spectra of pure HDA and pure LDA. As the sample is annealed further, it transforms completely to LDA.

In this study, we anneal HDA slowly at 1 bar, and make (1) annealed HDA without any LDA and (2) annealed HDA including the LDA component. We then measure their volume change during compression at 77 K. The V of non-annealed HDA, marked 2 in figure 6(b), decreases monotonically with increasing pressure. The annealed HDA without LDA, marked 3 and 4, begin to densify at ~0.80 and
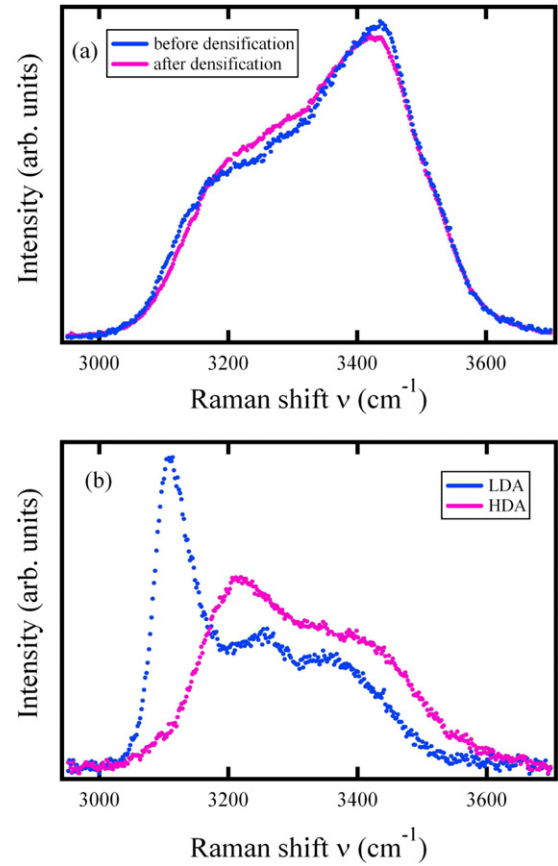
~0.67 GPa, respectively. Their densification behaviors are continuous and broad, and seem to depend on the initial HDA state before compression. This volume change is similar to the densification of the glassy $LiCl_{aq}$ solution, suggesting the structural relaxation of HDA.

We point out that this volume change of the annealed HDA without LDA resembles that of the HDA to very high-density amorphous ice (VHDA) transformation during compression at 135 K [19–21]; that is, VHDA is likely the densified HDA. This suggestion agrees with recent results of molecular dynamics simulations [22–24] that the HDA–VHDA transformation relates to structural relaxation from HDA to VHDA.

On the other hand, the detailed structural difference between HDA and VHDA and the continuous transformation between them are investigated by Loerting *et al* [19–21]. They propose that the HDA state differs from the VHDA state. Although a computer simulation predicts that a critical point relating to HDA and VHDA may exist [25], there is no direct experimental evidence of its existence yet. Future detailed investigations of HDA/VHDA will bring a better comprehension of the relation between HDA and VHDA.
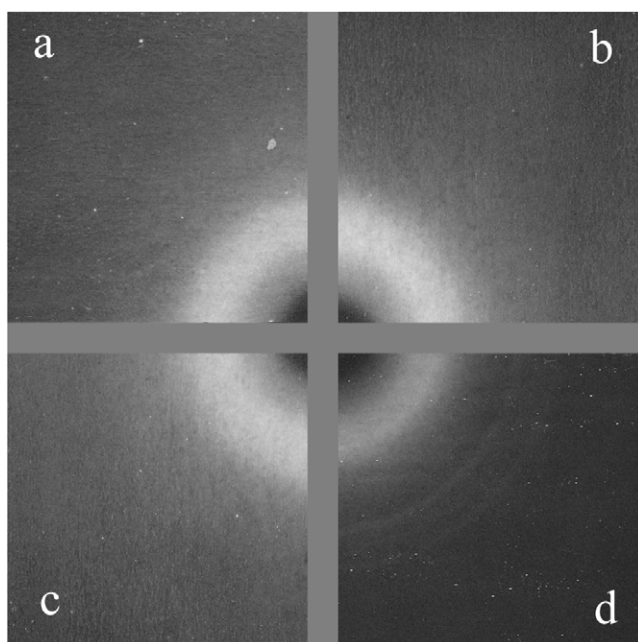
Figure 5. X-ray diffraction patterns of glassy LiCl$_{aq}$ solutions (a) before and (b) after the densification, (c) the densified glassy LiCl$_{aq}$ solution after the 1 bar annealing, and (d) crystalline ice Ic. In the x-ray measurements, we expose the sample placed in the liquid-nitrogen glass-vacuum flask to Zr-filtered Mo characteristic x-rays, and take a picture using Polaroid film. The film is exposed to the x-rays diffracted from not only the sample but also the liquid nitrogen and thin glass walls of the flask. All x-ray photos are taken at 77 K and 1 bar.

When the annealed HDA including the LDA component is compressed, its V decreases rapidly and discontinuously at $\sim$0.68 GPa, that is, the LDA–HDA transition pressure (figure 6(b)). This indicates that the LDA component transforms to HDA.

4. Conclusion

The volume change during the densification of glassy LiCl$_{aq}$ solution is broad and continuous, while the volume change during the LDA–HDA polyamorphic transition is sharp and discontinuous. Moreover, the Raman profiles before and after the densification are similar, while Raman profiles before and after the polyamorphic transition are distinctly different. In general, it is not clear whether the densification is a universal phenomenon for all glassy materials. The present experimental results show that the densification of glass relates to the structural relaxation of glass and differs intrinsically from the polyamorphic transition. This indicates that a stepwise volume decrease of glassy material does not necessarily mean a polyamorphic transition. We note that the volume change of polyamorphic transition can be continuous like that of densification because of non-equilibrium. Therefore, other evidence that the glassy states or structures before and after the volume change are drastically distinct should be at least necessary in order to recognize the polyamorphic transition. The distinct difference in structure would be
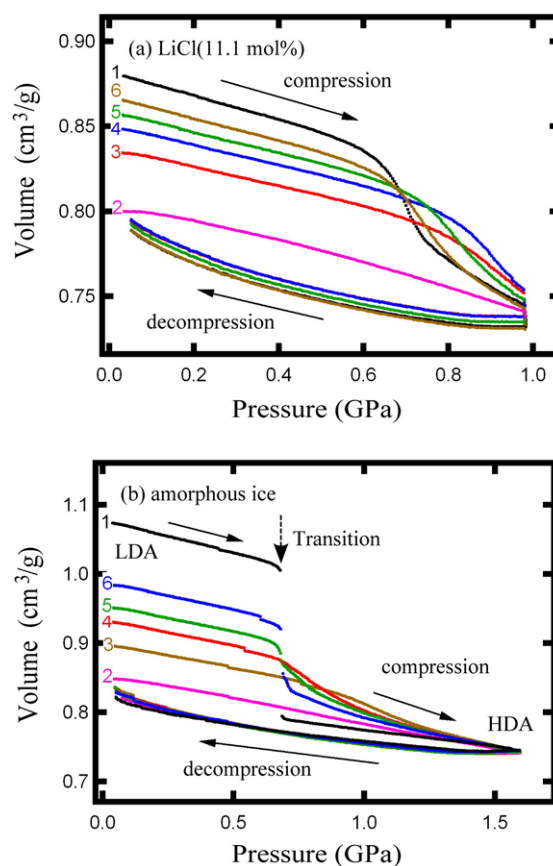

Figure 6. The annealing effects on the 77 K densification of glassy LiCl$_{aq}$ solution and the 77 K-LDA–HDA transition. (a) The P–V curve of glassy LiCl$_{aq}$ solution made by cooling to 77 K at 1 bar is marked 1. The non-annealed densified glassy solution is marked 2. The 1 bar annealed glassy solutions are marked 3–6. (b) The P–V curve of LDA at 77 K is marked 1. The transition from LDA to HDA occurs at 0.68 GPa (arrow). The non-annealed HDA is marked 2. The annealed HDA without LDA components are marked 3 and 4. The annealed HDA including LDA components are marked 5 and 6.

recognized by the appearance of new peaks in the Raman (or x-ray) spectra. According to the above differentiation of the polyamorphic transition, the HDA–VHDA transition appears to be a densification relating to structural relaxation.

References

[1] Dyre J C 2006 *Rev. Mod. Phys.* **78** 953
[2] Bridgman P W and Simon I 1953 *J. Appl. Phys.* **24** 405
[3] Mackenzie J D and Laforce R P 1963 *Nature* **197** 480
[4] Mackenzie J D 1963 *J. Am. Ceram. Soc.* **46** 461
[5] Brazhkin V V and Lyapin A G 2003 *J. Phys.: Condens. Matter* **15** 6059
[6] McMillan P F, Wilson M, Wilding M C, Daisenberger D, Mezouar M and Greaves G N 2007 *J. Phys.: Condens. Matter* **19** 415101
[7] Debenedetti P G 2003 *J. Phys.: Condens. Matter* **15** R1669
[8] Mishima O and Stanley H E 1998 *Nature* **396** 329
[9] MacFarlane D R, Scheirer J and Smedley S I 1986 *J. Phys. Chem.* **90** 2168
[10] Prével B, Jal J F, Dupuy-Philon J and Soper A K 1995 *J. Chem. Phys.* **103** 1886
[11] Mishima O 2004 *J. Chem. Phys.* **121** 3161

[12] Suzuki Y and Mishima O 2000 *Phys. Rev. Lett.* **85** 1322
[13] Moynihan C T, Easteal A J, Wilder J and Tucker J 1974
     J. Phys. Chem. **78** 2673
[14] Angell C A, Williams E, Rao K J and Tucker J C 1977 *J. Phys.
     Chem.* **81** 238
[15] Quach A and Simha R 1971 *J. Appl. Phys.* **42** 4592
[16] Eckstein A and Schneider H A 1996 *J. Therm. Anal.* **46** 973
[17] Finney J L, Hallbrucker A, Kohl I, Soper A K and Bowron D T
     2002 *Phys. Rev. Lett.* **88** 225503
[18] Mishima O and Suzuki Y 2002 *Nature* **415** 599
[19] Loerting T, Schustereder W, Winkel K, Salzmann C G,
     Kohl I and Mayer E 2006 *Phys. Rev. Lett.* **96** 025702

[20] Winkel K, Elsaesser M S, Mayer E and Loerting T 2008
     J. Chem. Phys. **128** 044510
[21] Bowron D T, Finney J L, Hallbrucker A, Kohl I, Loerting T,
     Mayer E and Soper A K 2008 *J. Chem. Phys.* **125** 194502
[22] Martoňák R, Donadio D and Parrinello M 2005 *J. Chem. Phys.*
     122 134501
[23] Martoňák R, Donadio D and Parrinello M 2004 *Phys. Rev. Lett.*
     92 225702
[24] Giovambattista N, Stanley H E and Sciortino F 2005 *Phys. Rev.
     Lett.* **94** 107803
[25] Paschek D, Rüppert A and Geiger A 2008 *ChemPhysChem*
     9 2737